

In vitro study to investigate effect of hypoxia on astroglial and neuronal co-cultures

Rasool, Rana Tahir

Master's thesis / Diplomski rad

2018

Degree Grantor / Ustanova koja je dodijelila akademski / stručni stupanj: **University of Zagreb, School of Medicine / Sveučilište u Zagrebu, Medicinski fakultet**

Permanent link / Trajna poveznica: <https://um.nsk.hr/um:nbn:hr:105:812487>

Rights / Prava: [In copyright](#) / [Zaštićeno autorskim pravom.](#)

Download date / Datum preuzimanja: **2025-01-28**



Repository / Repozitorij:

[Dr Med - University of Zagreb School of Medicine Digital Repository](#)



UNIVERSITY OF ZAGREB

SCHOOL OF MEDICINE

Rana Tahir Rasool

**In Vitro Study to Investigate Effect of
Hypoxia on Astroglial and Neuronal Co-
cultures**

Graduate Thesis



Zagreb, 2018

This graduate thesis was made at the Department of Histology and Embryology, mentored by Prof. dr. sc. Dinko Mitrečić and was submitted for evaluation in the academic year 2017/2018.

Abbreviations

AMPA	a-amino-3-hydroxy-5-methyl-4-isoxazolepropionic acid receptor
EGF	Epidermal growth factor
FBS	Fetal bovine serum
FGF-2	Fibroblast growth factor-2
GFAP	Glial fibrillary acidic protein
HIF-1	Hypoxic inducible factor-1
IVT	Intravenous thrombolysis
MLKL	Mixed lineage kinase domain like pseudokinase
NMDA	N-methyl-D-aspartate receptor
Nogo	Neurite outgrowth inhibitor
NSCs	Neural stem cells
PBS	Phosphate buffered saline
PDL	Poly-D-lysine
rt-PCR	real-time polymerase chain reaction
TNF	Tumor necrosis factor

Table of Contents

1. Abstract	1
2. Sažetak	2
3. Introduction	2
4. Hypothesis	6
5. Objectives of the study	6
6. Experiment design	7
7. Materials and Methods	8
7.1. Primary astrocyte cultures.....	8
7.2. Neuronal stem cells (NSCs) cultures	8
7.3. Cells cultivation and seeding	9
7.4. Live-cell imaging and cell tracing	10
7.5. Immunocytochemistry	11
7.6. RNA isolation for real time-PCR.....	12
7.7. Real time-polymerase chain reaction.....	12
8. Results	14
8.1. Characterization of neuronal differentiation of neural stem cells in normoxia	14
8.2. Characterization of neuronal differentiation of neural stem cells in hypoxia.....	14
8.3. Characterization of astroglial-neuronal co-cultures in hypoxia.....	15
8.4. Quantification of cellular motility in normoxia and hypoxia	16
8.5. Relative expression of caspase 8 and MLKL in astroglial-neuronal co-cultures in normoxia and hypoxia.....	20
9. Discussion	20
10. Conclusion	24
11. Acknowledgment	25
12. References	26
13. Biography	31

1. Abstract

Introduction: Stroke is the second most common cause of death in the world and 85% of strokes are ischemic due to obstruction of blood vessels. This leads to deprivation of oxygen and glucose, which causes energy failure and neuronal death. There is an increasing interest in developing new therapies for ischemic stroke due to short therapeutic window and lack of currently available treatments. Astrocytes provide a major role in brain's response to ischemic injury by providing antioxidant protection, growth factors and glutamate clearance. A detailed understanding of astrocyte-neuron interaction can provide valuable therapeutic targets. This study aims to use astroglial-neuronal co-cultures to investigate affect of hypoxia on interaction between astrocytes and neurons.

Methods: Primary astrocytes were obtained from mouse newborns and NSCs from E14.5 mouse embryos. Astrocytes and NSCs were seeded together to develop astroglial-neuronal co-cultures, which were incubated in normoxic and hypoxic conditions. Co-cultures were characterized using live imaging and immunocytochemistry, quantification of cellular motility and relative gene expression of apoptotic (caspase 8) and necroptotic marker (MLKL) was performed using live cell tracing and rt-PCR respectively.

Results: The characterization of co-cultures in hypoxic conditions showed NSCs differentiation into unipolar and bipolar neurons and presence of flat and epithelioid astrocytes. The average and maximum speed of cells in astroglial-neuronal co-cultures was higher in hypoxic conditions, but less than NSCs single culture in normoxia. Relative gene expression of caspase 8 was higher than MLKL in both hypoxic and normoxic conditions.

Discussion: There was better differentiation and survival of NSCs in astroglial-neuronal co-cultures in hypoxic conditions. This was also reflected in better cellular motility of astroglial-neuronal co-cultures in hypoxic conditions. Caspase 8 and MLKL exhibited reciprocal relationship of expression in both normoxic and hypoxic conditions. Although we observed difference in expression of caspase 8 and MLKL in normoxic and hypoxic conditions, more samples will be needed to define precise levels of statistical significance of this finding.

Conclusion: In this work we observed responses of astrocytes and neurons in astroglial-neuronal co-cultures, which were fairly consistent with what happens in ischemia. More studies will be required to characterize and understand observed phenomena in the astroglial-neuronal co-cultures.

Key Words: Astrocytes, neuronal stem cells (NSCs), astroglial-neuronal co-cultures, hypoxia, cell motility, caspase 8, MLKL, real-time PCR.

2. Sažetak

Uvod: Moždani udar je drugi najčešći uzrok smrti u svijetu. U 85% slučajeva se radi o ishemijskom moždanom udaru uzrokovanom prekidom protoka krvi, a time glukoze i kisika, kroz krvnu žilu, što uzrokuje energetske disbalans i smrt neurona. Trenutno dostupni terapijski pristupi mogu se primjeniti u ograničenom vremenskom razdoblju te stoga postoji potreba za novim pristupima u liječenju ishemijskog moždanog udara. Astrociti imaju važnu ulogu u odgovoru na ishemiju mozga jer pružaju antioksidativnu zaštitu, proizvode faktore rasta te uklanjaju glutamat. Bolje poznavanje interakcija između neurona i astrocita moglo bi iznjedrili neke nove terapijske mete. Cilj ovog rada je bio uspostaviti kokulture astrocita i neurona te istražiti utjecaj hipoksije na interakciju astrocita i neurona.

Metode: Primarni astrociti izolirani su iz novorođenih miševa, dok su živčane matične stanice izolirane iz embrija miševa starih 14.5 dana. Astrociti i živčane matične stanice su nasađeni zajedno kako bi se dobila mješovita kultura, uzgajana u normalnim uvjetima te u uvjetima hipoksije. Mješovite kulture su analizirane imunohistokemijski, praćena je mobilnost stanica i analizirana je ekspresija apoptotičkog (*Casp8*) i nekroptotičkog markera (*Mkl*) metodom qRT-PCR.

Rezultati: Karakterizacija mješovitih kultura u hipoksičnim uvjetima pokazala je da su se živčane matične stanice diferencirale u unipolarne i bipolarne neurone te je pokazana prisutnost plosnatih i elipsoidnih astrocita. Vrijednosti prosječne i maksimalne brzine stanica u mješovitim kulturama su bile veće u hipoksičnim uvjetima, ali manje od onih zabilježenih u kulturi samih živčanih matičnih stanica u normalnim uvjetima. Relativna ekspresija gena *Casp8* bila je veća od ekspresije *Mkl* i u hipoksičnim i normalnim uvjetima.

Diskusija: U hipoksičnim uvjetima zabilježena je bolja diferencijacija i preživljenje živčanih matičnih stanica te bolja mobilnost stanica u kokulturi. Iako je zabilježena razlika u relativnoj ekspresiji gena *Casp8* i *Mkl* u normalnim i hipoksičnim uvjetima, za određivanje razine statističke značajnosti će biti potrebno imati veći broj bioloških replika.

Zaključak: U mješovitoj kulturi astrocita i neurona smo opazili promjene koje se inače dešavaju u ishemiji. Potrebna su nova istraživanja na ovim stanicama koja će dovesti do boljeg razumijevanja interakcija prisutnih u hipoksiji.

Ključne riječi: Astrociti, NSC (živčane matične stanice), kokultura astrocita i neurona, mobilnost stanica, *Casp8*, *Mkl*, qRT-PCR.

3. Introduction

Stroke is the second most common cause of death in the world and one of the main causes of disability in adults. In 2013, there were 6.5 million deaths due to stroke, and with an overall cost of 113 million disability-adjusted life years (1) The burden of stroke due to illness, disability and early death is set to double worldwide within next 15 years due to rise in prevalence of vascular risk factors in developing countries (1). Stroke can be divided into two main types, ischaemic and haemorrhagic. Ischemic stroke accounts for 85% of strokes, and it results from vascular occlusion, due to atherosclerotic large artery disease, small artery disease (lacunar infarcts), or cardioembolic events (2). The treatments for ischemic stroke are neuroprotective, that target to prevent the brain damage due to vessel occlusion and neurorestorative, which aim to repair the brain damage after it has already been done.

Within minutes after the blockage of an artery, the “necrotic core” develops where brain tissue is irreversibly damaged. The reversible damaged tissue “ischemic penumbra” around the necrotic core receives inadequate blood flow from the collateral bloody supply (3). The central goal of therapy in acute ischemic stroke today is to preserve tissue in the ischemic penumbra by restoring the blood flow to it before irreversible cell damage has occurred (4). Currently, the standard of care treatment in acute ischemic stroke is neuroprotective intravenous thrombolysis (IVT). In IVT, recombinant tissue-type plasminogen activator (rt-PA) is intravenously administered in order to break down the blood clot and restore the blood flow to ischemic penumbra (5). Despite strong evidence that IVT improves outcomes in acute ischemic stroke, it has notable limitations of hemorrhagic transformation (6), narrow therapeutic time window of 4.5 to 6 hours (5), and ineffectiveness in lysing big clots (7). Further, due to contraindications of IVT, only up to 24% of acute ischemic patients can be eligible for IVT if treatment is not delayed (8). In last few years, multiple clinical trials have shown evidence in support of acute endovascular thrombectomy using stent-retriever for the treatment of acute ischemic stroke (9). However, it is also restricted to only a small portion of patients, due to contraindications, short therapeutic window and the costs associated with establishing the infrastructure to deliver this treatment (10).

The cell death in ischemic stroke starts within few minutes after the vessel occlusion, longtime before the clot can be removed. One key mediator of cell death in ischemic stroke is excitotoxicity as a consequence of adenosine triphosphate (ATP) depletion and failure to

maintain membrane potentials. This results in excessive release of glutamate, which in turn leads to activation of ionotropic glutamatergic receptors (AMPA, Kainate and NMDA). The activation of these receptors leads to uncontrolled calcium entry which disrupts a vast variety of physiological processes, ultimately resulting in DNA, lipid and protein damage and eventually cell death (11). A number of neuroprotective agents targeting excitotoxicity have been tried to limit the cell death during an ischemic stroke. The NMDA antagonists targeted against excitotoxicity have failed to demonstrate benefits in patients (12). The animal studies have shown that targeting the downstream pathway of excitotoxicity can be of clinical importance. Coupling of activated subunit (NR2B) of NMDA receptor with death associated protein kinase1 (DAPK1), during excitotoxicity results in apoptosis. Inhibition of this coupling by a compound called NR2B_{CT} or by interfering with p53 signaling pathway can reduce infarct size and improve neurological outcome in animal models (13, 14).

A peptide called NA-1 is another example of neuroprotective therapy that targets downstream pathway of excitotoxicity. NA-1 works by inhibiting the coupling of NMDA receptor subunits (PSD)-96 and neuronal nitric oxide synthase (nNOS). This uncoupling of nNOS from activated glutamate receptor leads to decrease production of noxious nitric oxide (NO) during excitotoxicity (15). A study done in three non-human primate models of ischemic stroke demonstrated neuroprotective role of NA-1 (16). A multicentre, randomized, double blind, placebo-controlled, phase III clinical trial using pre-hospital administration of NA-1 in ischemic stroke is currently recruiting. The primary objective is to determine the efficacy of NA-1 in reducing global disability in patients with acute ischemic stroke. The secondary objectives are to determine the effectiveness of NA-1 in reducing functional dependence, improving neurological outcome, improving activities of daily living, and increasing the proportion of subjects who are candidates for endovascular recanalization therapy (17).

The generation of free radicals, including reactive oxygen and nitrogen species (ROS/RNS), during ischemia is another key step to cell death in brain during an ischemic injury (18). Pre-clinical studies showed that limiting the production of these free radicals could have neuroprotective effect in decreasing the brain damage due to ischemic-reperfusion injury (15). Though, the results of these pre-clinical studies are yet to be translated into clinical practice. The clinical trials of NXY-059, a nitrogen free radical scavenger, and uric acid failed to demonstrate benefit in ischemic stroke patients (19, 20). Edaravone, another

scavenger compound, is clinically used in parts of Asia and meta-analyses of trials suggest it reduces neurological impairment; however, it is not used in Europe or America due to lack of clinical evidence from a large phase III trials in non-Asian populations (21).

Due to short therapeutic window and unsuccessful clinical trials of neuroprotective therapies to minimise the tissue infraction, there is an increasing interest of current research to develop neurorestorative therapies for treating stroke after the damage has been done (22). Neurorestorative agents amplify endogenous brain repair mechanisms to repair damaged tissue. Neurorestorative therapies have the advantage of long therapeutic window and could be given as stand-alone or as an adjunct therapy to improve stroke outcome. Preclinical data indicate that cell-based and pharmacological therapies that enhance brain-repair processes substantially improve functional recovery when given 24 h or later after stroke (23). It is proposed that cell-based therapies, including mesenchymal cells, bone marrow cells and neuronal stem cells stimulate the production of restorative factors by endogenous parenchymal cells leading to enhancement of endogenous neurogenesis in brain after ischemia (24). A phase I clinical trial of allogenic neural stem cells (NSCs) in patients with chronic ischemic stroke has shown no adverse events and improved neurological functions (25). Neurorestorative therapies that targeted against inhibitors of neuronal growth such as myelin-associated glycoprotein, the Nogo family of proteins, and chondroitin sulphate proteoglycans in the glial scar did not show clinical benefit (26).

While most of the research has been directed towards at preventing direct neuronal death or affecting neuronal repair, a considerable amount of damage caused to brain tissue after ischemic stroke is due to inflammation. The activation of the immune system after ischemic stroke has been described as a double-edged sword, with microglia actively removing dead cells but also producing toxic substances that potentially exacerbate damage (27). The protective role of microglia is associated with their activation in the absence of “off” signal from neurons via ligand-receptor interaction during ischemia that is usually present in normal conditions (28). On the other hand, toxic character of microglia is related to their activation by damage-associated molecular patterns (DAMPs) via toll-like receptors during ischemia (29). The therapeutic approaches that have targeted the reduction of toll-like receptor signalling are known to reduce lesion volume in ischemic animal models (30, 31). The results of a clinical trial showed that oral administration of minocyclin, a second-generation

tetracycline, within 6 to 24 hours after acute ischemic stroke for 5 days significantly improved stroke outcome (32). The mechanism of minocycline induced neurorestorative effect is related to reduction of inflammation induced by activated microglia (33).

Astrocytes are the most abundant cell type in mammalian brain and play a major role in brain's response to all types of injuries including ischemic stroke. In the setting of ischemia, astrocytes perform multiple functions, some beneficial and some potentially detrimental. The astrocyte syncytium provides a network of communication channels called gap junctions throughout the brain. Following ischemic stroke, the gap junctions remain open allowing propagation of damaging spreading depression (34). Activated astrocytes also produce proinflammatory cytokines, which can be detrimental to ischemic recovery by inducing apoptosis of neuronal cells (35). The reactive astrocytes form a glial scar around the infarct area over many weeks after the injury, and studies have established that the glial scar helps to provide a barrier to localise the damage within the brain, but in doing so it also becomes a physical and chemical barrier for axonal regeneration (36).

Astrocytes support neurons during ischemic injury by providing antioxidant protection, substrates for neuronal metabolism, growth factors and glutamate clearance (37). The neurons die in ischemic penumbra when native astrocytes undergo programmed cell death or become malfunctioning leading due delayed expansion of the evolving infarct (37, 38). Therefore, many recent efforts have focused on the astrocyte-neuron interaction and how astrocyte function can be improved after stroke to enhance neuronal support and survival (39, 40). A detailed understanding of astrocyte-neuron interaction can provide valuable therapeutic targets to develop both neuroprotective and neurorestorative treatments for ischemic stroke patients. The use of co-cultures in *in vitro* model, where astrocytes and neurons are grown together allowing physical contact between each other, constitute valuable tool to study the interaction between cell populations. An *in vitro* model of cell cultures has the advantage of controllability and ability to provide detailed basic information on how a particular cell population responds to specific stimuli or insult (41).

4. Hypothesis of the study

In vitro model of astroglial-neuronal co-cultures will allow to obtain detailed insight in the processes occurring in the nervous tissue in regard to normoxic and hypoxic conditions.

5. Objectives of the study

The aim of this study was to develop an *in vitro* model of astroglial and neuronal co-cultures, which can then be utilized to study the interaction between astrocytes and neurons during normoxic and hypoxic conditions:

5.1 Qualitative data: To illustrate neuronal differentiation of NSCs to neurons with neuronal differentiation medium, and to characterise astroglial and neuronal co-cultures in hypoxic conditions using immunohistochemistry and live-cell imaging.

5.2 Quantitative data: To quantify locomotion of cells in astroglial and neuronal co-cultures during normoxic and hypoxic conditions using live-cell imaging and cell tracking software. To determine if apoptosis or necroptosis is the main process of cell death in astroglial-neuronal co-cultures due to hypoxia by measuring relative gene expression of apoptotic (caspase 8) and necroptotic marker (MLKL) with rt-PCR.

6. Experiment design

Primary astrocytes were obtained from cerebral cortices of newborns and NSCs were isolated from telencephalon wall of E14.5 and E15.5 mouse embryos. Neurons were developed from NSCs by adding neuronal differentiation medium. Astrocytes and NSCs were seeded together with astrocyte growth medium and neuronal differentiation medium to create astroglial-neuronal co-cultures. Controls and co-cultures were incubated in normoxic and hypoxic conditions. Subsequently live-cell imaging, immunocytochemistry, cell tracking and rt-PCR were performed to obtain data. Figure 1 shows the experiment design in detail.

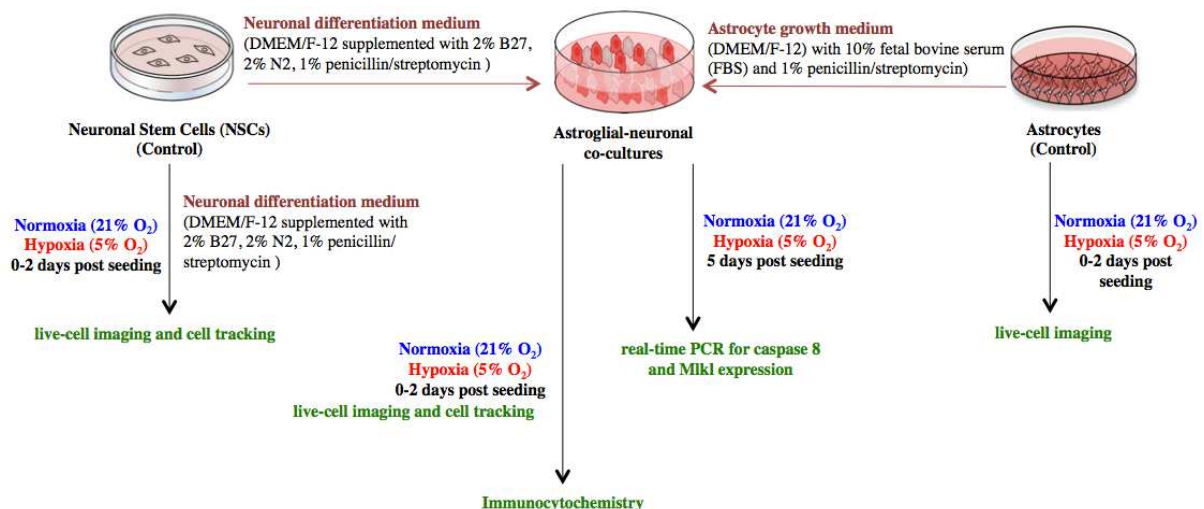


Figure 1: Schematic diagram of experiment design of this study.

7. Materials and Methods

7.1. Primary astrocytes cultures

Primary astrocytes were isolated from the cerebral cortices of six newborn pups of mouse strain B6.Cgp-Tg (Thy1-YFP) 16Jrs/J. Briefly, the heads of embryos were decapitated at the level of cervical spine and submerged in 70% ethanol for disinfection. The decapitated heads were taken out of ethanol and placed in petri dishes containing 1x phosphate buffered saline (PBS). The brains were exposed after removing the skin and cranium. The cerebral cortices were isolated from exposed brains after removing the meninges and white matter. The cerebral cortices were chopped into small pieces, and pooled together in 50ml falcon tube. The warm 0.1% trypsin was added to the pooled cortices and incubated in 37 °C for 20 minutes, and mechanical dissociation of the cerebral cortices was performed to reach the homogenous fluid. The warm DMEM/F-12, to stop the action of trypsin, was added to homogenous fluid containing cells and trypsin, and centrifuged at 400 x g for 6 minutes at room temperature. After discarding the supernatant, the pellet of cells was re-suspended and dissociated in astrocyte cell culture medium (DMEM/F-12 supplemented with 10% fetal bovine serum (FBS) and 1% penicillin/streptomycin). The cells with culture medium were transferred to 75 cm² flask and placed in a 37 °C incubator at 5 % CO₂. The metabolic activity of astrocytes is higher compared to other cell types such as microglia; therefore, in nutritionally deprived conditions astrocytes show low survival rate while microglia is not affected by nutritional deprivation and proliferate in such conditions (42). Further, astrocytes tend to attach to surface of flask and grow as monolayer, while the microglia grow freely on top of the astrocytic cell monolayer (43). To maintain low number of microglial cells in astroglial cultures, the astrocyte culture medium was changed every 3 days to prevent nutritional deprivation conditions and to remove free growing microglia. The cells were grown to confluence before seeding.

7.2. Neuronal stem cells (NSCs) cultures

Neuronal stem cells (NSCs) were isolated from telencephalon wall of E14.5 and E15.5 embryos of mouse strain B6.Cgp-Tg (Thy1-YFP) 16Jrs/J. Briefly, the pregnant females were euthanized with cervical dislocation. Following the disinfection of abdominal area with 70% alcohol, uterus was surgically removed and placed in cold PBS. The embryos were removed from the uterus and placed in a Petri dish with cold PBS. The heads of embryos were severed at the level of cervical spine, and cerebral cortices were isolated while white matter and meninges were removed. The cortices were chopped into small pieces and pooled together in

50ml falcon tube. The warm accutase was added to the pooled cortices and incubated in 37 °C for 20 minutes. The cortices were mechanically dissociated well to obtain turbid fluid. The warm DMEM/F-12 was added and centrifuged at 400 x g for 6 minutes at room temperature. The pallet containing cells was re-suspended and dissociated in full NSC medium (DMEM/F-12 supplemented with 2% B27, 2% N2, 1% penicillin/streptomycin, and 20ng/ml final concentration of each; fibroblast growth factor (FGF-2) and epidermal growth factor (EGF)). The cells with full NSC medium were transferred to 75 cm² flasks and placed in a 37 °C incubator at 5 % CO₂.

7.3. Cells cultivation and seeding

NSCs with neuronal differentiation growth medium were seeded in 24 well plate pre-coated with polydellisine (PDL) and laminine in normoxic and hypoxic conditions for live-cell imaging. Astrocytes and astroglial-neuronal co-cultures were grown on PDL and laminine coated glass coverslips placed in the 24 well plates in normoxic and hypoxic conditions for live-cell imaging and immunocytochemistry. To measure gene expression using rt-PCR, astroglial and neuronal co-cultures were seeded in 6 well plates, in both normoxic and hypoxic conditions.

Coating of glass coverslips with PDL and laminine: Glass coverslips were placed in a petri dish, and HNO₃ added. The petri dish was wrapped with aluminum foil and left overnight on the shaker (30 rpm) at room temperature. The next day, HNO₃ was removed and coverslips were rinsed with sterilized water for 2 hours at room temperature on the shaker. Then coverslips were rinsed in 70% ethanol at room temperature and left on the shaker for overnight. Following day, ethanol was removed and the petri dish with coverslips was placed at 250 °C for 8 hours. The sterilized coverslips were placed carefully in 24-well plate, each per well. Prepared solution of PDL (Ploy-D-lysine hydrobromide, 5mg/50 ml P6407-5MG, Sigma) was added over the surface of sterilized coverslip in each well and incubated overnight at room temperature in the cell culture hood. Next day, PDL solution was aspirated and coverslips were washed 3 times by sterilized water. Then prepared solution of laminine (1mg/ml Catalyst L2020-1MG, Sigma) was added to coverslips at +4 °C for overnight. Before the cell seeding, laminine was aspirated from each well and coverslips were washed 2 times with 1x PBS.

Astrocytes cultivation and seeding: Primary astrocytes cultures were used to seed astrocytes. Astrocytes were cultivated by adding 0.1% warm trypsin in 75cm² flask containing astrocytes after removing the culture medium from it. Trypsin was added for cell detachment from the surface of flask. Warm DMEM was added to stop the reaction of trypsin. Cells along with trypsin and DMEM were collected in a falcon tube and spun at 400g for 6 minutes. After removing the supernatant, the cell pellet was dissociated in full astrocytic culture medium (DMEM/F-12 supplemented with 10% FBS and 1% penicillin/streptomycin). The cell density was determined by staining cells in trypan blue and counting with cytometer under the light microscope. Approximately, 50,000 cells per well were seeded with full astrocyte culture medium.

NSCs cultivation and neurons seeding: NSCs cultures grown to neurospheres were used to seed neurons. NSCs were cultivated from neurospheres by adding warm accutase. Accutase was added to dissociate the neurospheres. Warm DMEM was added to stop the reaction of accutase. Cells, accutase and DMEM were collected in a falcon tube and spun at 400g for 6 minutes. The supernatant was discarded and cell pallet was suspended in neuronal differentiation medium (DMEM/F-12 supplemented with 2% B27, 2% N2, 1% penicillin/streptomycin). The lack of growth factors (FGF-2 and EGF) in growth medium causes differentiation of NSCs into neurons. The cell density was determined by staining the cells in trypan blue and counting with cytometer under the light microscope. Approximately, 50,000 cells were seeded per well with neuronal differentiation medium.

Astroglial and neuronal co-cultures seeding: To create astroglial and neuronal co-cultures, astrocytes and NSCs were cultivated from primary astrocytes culture and primary NSCs culture as described above. First astrocytes were seeded and allowed to attach to the surface for few hours. Then NSCs were seeded in the same well. Each cell types were seeded with approximately 50,000 cells per well. The growth medium for astrocytes (DMEM/F-12) with 10% FBS and 1% penicillin/streptomycin) and neuronal differentiation medium (DMEM/F-12 supplemented with 2% B27, 2% N2, 1% penicillin/streptomycin) were added in each well in 50/50 ratio.

7.4. Live-cell imaging and live-cell tracing

Astrocytes, NSCs-neurons, astroglial and neuronal co-cultures were incubated in the cell chamber of EVOS FL Auto Cell Imaging System from Thermo Fisher Scientific for live imaging. The conditions for cells were normoxic (21% O₂) and hypoxic (5% O₂), both at 37

$^{\circ}\text{C}$ in 5% CO_2 . The cells were placed in these conditions for 72 hours (Day 0, 1, 2) and live images were taken at 20x magnification for every 7 minutes at different beacons for each condition. The live images were made into stacks by using ImageJ. The stacks were used to track the cells with software called CellTracker written in MatLab 2012. The data was obtained from the CellTracker software about parameters (maximum speed, average speed and average angle of direction from origin) of locomotion of cells. Statistics were performed on the results acquired from the CellTracker using GraphPad Prism.

7.5. Immunocytochemistry

The cells used in the immunocytochemistry assays were cultured in 24 well plates containing coverslips previously coated with PDL and laminine. After removing the culture medium, the cells were rinsed with 1x PBS and fixed in 4% paraformaldehyde for 10 min at room temperature. For blocking non-specific antibody binding and cell permeabilization, cells were incubated with blocking buffer (3 % bovine serum albumin (BSA), 3% donkey serum albumin (DSA) in 1x PBS) and 0.2% triton x-100 combined with blocking buffer for 3 hours at room temperature. The cells were incubated overnight at 4 $^{\circ}\text{C}$ with anti-gial fibrillary acidic protein (chicken anti-GFAP; 1:250; ab4674), anti-microtubule-associated protein 2 (chicken anti-MAP2; 1:1000; ab5392), anti-antigen Ki67 (rabbit anti-Ki67; 1:250; ab15580), anti-nestin (goat anti-nestin; 1:500; sc-21248) and anti-CD11b (rabbit anti-CD11b; 1:300&1:500; ab133357) diluted in blocking buffer and 0.2% triton x-100. The neuronal-astroglial co-cultures and astrocytic cultures, both in normoxia and hypoxia, were stained with combinations of GFAP+Ki67, MAP-2+Ki67, nestin+Ki67, nestin+GFAP and nestin+MAP. The astrocytic cultures in normoxia conditions were also stained with CD11b+GFAP to examine the presence of microglia. After removing the primary antibodies, cells were washed 3x5min with PBS. Then cells were incubated with secondary antibodies: goat-anti-chicken conjugated to Alexa Fluor 546 (1:1000; A11040), donkey-anti-goat conjugated with Alexa Fluor 546 (1:1000; A11056), donkey-anti-rabbit conjugated with Alexa Fluor 488(1:1000; A21206) and donkey-anti-goat conjugated to Alexa Fluor 488 (1:1000; A11055) diluted in 1x PBS for 1 hour at room temperature. After removing the secondary antibodies, the cells were washed 3x5min with 1x PBS and incubated for 10 min with nuclear marker, Hoechst/Dapi (1:8000; Roche; 10236276001) diluted in 1x PBS. After removing the nuclear marker, the cells were washed again 3x5min with 1x PBS. The cover slip containing stained cells was removed from the 24 wells plate, and mounted onto glass slide in Dako fluorescence mounting medium. Images were acquired using EVOS FL Auto

Cell Imaging System with 40x objective. Images were processed by software called ImageJ.

7.6. RNA isolation for real time-PCR

RNA was isolated from astroglial-neuronal co-cultures incubated in normoxic and hypoxic conditions for 5 days. The protocol was adapted from the one provided with the RNeasy mini kit (Qiagen, cat no. 74104). Briefly, the cell culture medium was removed and the cells were washed with 1x PBS. The RLT buffer was added in each well, which lysed the cells and released RNA. The RLT buffer also inactivated RNase to ensure purification of intact RNA. The lysed cells were scraped off from surface of the plate by the cell scraper, and collected in small Eppendorf tubes. The collected cells were spin at 14000 x g for 3 minutes, and 70% ethanol was added. The centrifuged cells with ethanol were transferred to RNeasy spin columns placed in a 2ml collection tube, and spun 2x for 15 seconds. The mRNA specifically bound to the silica-based membrane in spin columns and contaminants were discarded which flow through into collection tube. The RW1 and RPE buffer were respectively added into spin columns and centrifuged for 15 seconds. The centrifugation was performed for 2 minutes with RPE buffer and for 1 minute without any buffer to ensure that no ethanol and buffer was carried over during RNA elution. The flow through from these centrifugations was discarded. The RNeasy spin columns were transferred into new 1.5 ml collection tubes. The RNase-free water was added directly to the spin columns membrane and centrifuged for 1 minute at 14000 rpm to elute the RNA. The RNA containing flow through was added again into the RNeasy spin columns membranes and centrifuged for one minutes at 14000g. The mRNA sample in the collected tubes was stored in -80 °C.

7.7. Real time-polymerase chain reaction

RNA was reverse transcribed into cDNA using a commercially available kit: a high capacity RNA-to-cDNA Kit (Applied Biosystems, 850 Lincoln Center Drive, Foster City, CA 94404, USA) according to the manufacturer's instructions and 27020 Thermal Cycler (Applied Biosystems) (44). The essays used in this study were Caspase 8 (Mm01255716_m1) and Mik1 (Mm01244222_m1) (TaqMan Gene Expression Assays), and gene expression was analyzed with respect to the endogenous control of beta-actin (ACTB MGB 4352933E) (TaqMan Gene Expression Assays). All samples were made in duplicates with 1 µg of cDNA in a total volume of 20 µL, and the chain reaction in real time was made according to the manufacturer's instructions and in the Applied Biosystems 7500 Real-Time PCR System.

The Applied Biosystems™ TaqMan® Real-Time PCR Exercise is based on following mechanism. The assays contain: a pair of unlabeled primers specific to the genome and probes with FAM™ or VIC™ fluorogenic colors at the 5' end, while at the 3' end of the small groove binder molecule (MGB) and a non-fluorescent molecule that captures the signal of a nonfluorescent quencher (NFQ). At the beginning of the polymerase chain reaction in real time, the temperature was raised to denature the double-stranded cDNA. During the first step, the fluorescence signal at the 5' end of the NFQ probe is captured at the 3' end and the signal can not be detected. In the next step, the reaction temperature is lowered to allow initiation and probe binding to complementary sequences in the cDNA. Taq DNA polymerase synthesizes new DNA lancing using uninitiated primers. When the polymerase reaches the labeled probe, its endogenous 5' nuclease activity breaks down the test by separating the color of the molecule that captures the color signal. With each cycle of polymerase chain reaction, more and more colors are released which results in an increase in the fluorescence intensity proportional to the synthesized amplicon.

The device measures the intensity of the fluorescence in each cycle whereby the so-called amplification curve is generated. At the amplification curve there is a threshold value, which is the value of the intensity of the fluorescence on which the signal obtained by amplification of the desired gene increases the initial noise. For the gene expression analysis, the number of cycles (CTs) that is found in the amplification curve between the signal boundary limit and the platinum that occurs when the reagents are consumed, i.e., there is no more amplification of the gene, so the fluorescence intensity is constant. The gene expression analysis was performed in such a way that the CT value of the endogenous control (beta actin) was deduced from the CT value for a given gene and a Δ CT value was obtained. Relative expression of the gene was obtained by the formula $2^{-\Delta CT}$.

8. Results

8.1. Characterization of neuronal differentiation of neural stem cells in normoxia

Images taken right after seeding of NSCs in normoxic conditions revealed that cells exhibit different morphology which were consistent with undifferentiated neuronal stem cells and neuronal progenitor cells with round and bi-polar shape, respectively (Figure 2). Due to neuronal differentiation medium, images taken 24 hours post-seeding showed the differentiation of NSCs into neurons with bi-polar and uni-polar morphology. Pyknotic cells with condensed nuclei can also be seen after 24h post-seeding of NSCs (Figure 3).

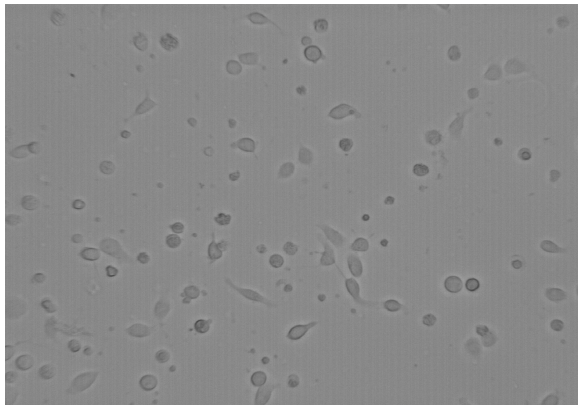


Figure 2: Image was taken 0h after seeding of NSCs in normoxic conditions. Cells with undifferentiated morphology of NSCs and neuronal progenitor cells can be seen.

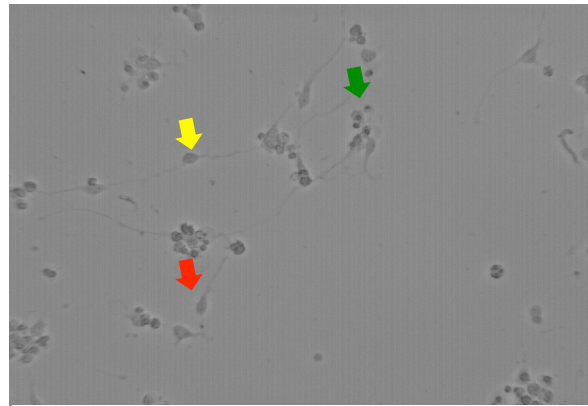


Figure 3: Image was taken 24h after seeding of NSCs in normoxic conditions. Yellow, red and green arrows show neurons with bi-polar and uni-polar morphology and pyknotic cells respectively.

8.2. Characterization of neuronal differentiation of neural stem cells in hypoxia

Immediately after seeding of NSCs in hypoxic conditions, images showed similar morphology of undifferentiated NSCs and progenitor cells as seen in normoxic conditions (Figure 4). At 24h post seeding, we observed neuronal differentiation: neurons with bi-polar and uni-polar morphology were seen. We observed more pyknotic cells in hypoxic conditions as compared to normoxic conditions (Figure 5).

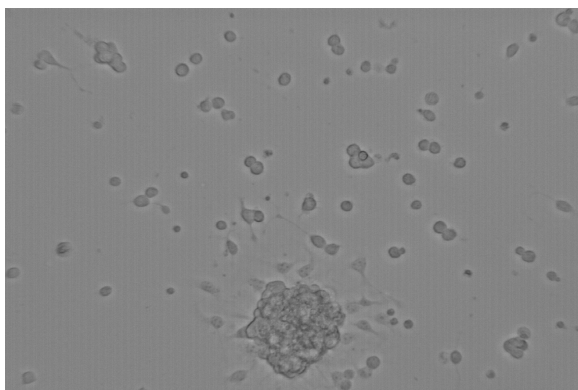


Figure 4: 0h after seeding of NSCs in hypoxic conditions. A neurosphere can be seen.

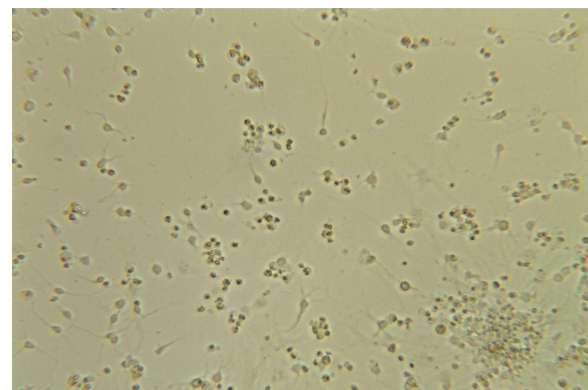


Figure 5: 24h after seeding of NSCs in hypoxic conditions. Neuronal differentiation was present.

8.3. Characterization of astroglial-neuronal co-cultures in hypoxia

Image taken after seeding of NSCs and astrocytes to create astroglial-neuronal co-cultures showed immature astrocytes attached to the surface and NSCs with round shape consistent with undifferentiated morphology (Figure 6). After 24h post seeding, astrocytes started to grow to confluence with flatter morphology and the physical contact between them was observed. There was also neuronal differentiation occurring, but it was less robust as compared to NSCs grown alone as seen in figure 3 and 5. There was physical contact between neurons and astrocytes. There were few pyknotic cells seen at 24h in astroglial-neuronal co-cultures (Figure 7).

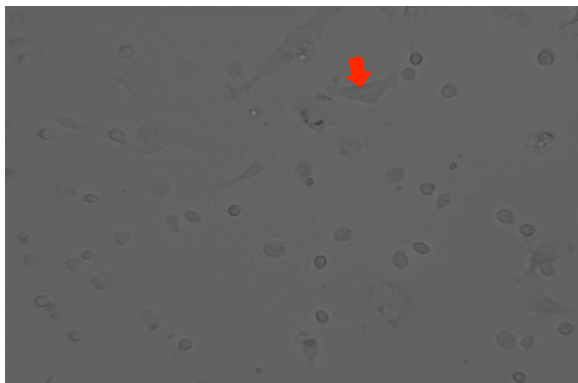


Figure 6: Image of astroglial-neuronal co-cultures at 0h after exposure to hypoxic conditions. Immature astrocytes (red arrow) and NSCs and neuronal progenitor cells were present.

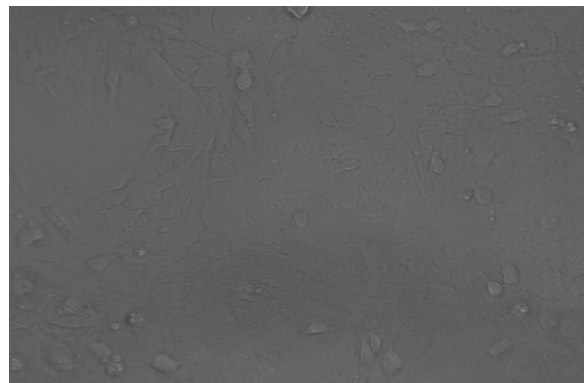


Figure 7: Image of astroglial-neuronal co-cultures at 24h after exposure to hypoxic conditions. There was physical contact between astrocytes-astrocytes and astrocytes-neurons.

Immunocytochemical images of astroglial-neuronal co-cultures after exposure to hypoxic conditions demonstrated presence of GFAP positive astrocytes and nestin positive cells (Figure 8 & 9). The morphology of astrocytes was broad and there were no elongated processes. There were also cells present positive for both nestin and Ki67, which demonstrated presence of dividing cells in hypoxic conditions (Figure 10).

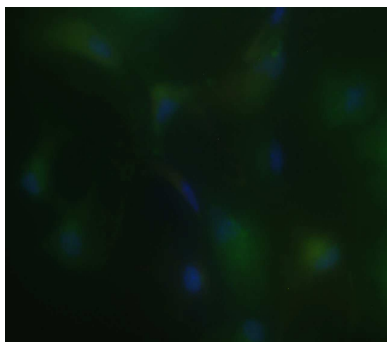


Figure 8: GFAP immunostaining showing astrocytes in co-cultures in hypoxic conditions. DAPI (blue) staining shows nuclei.

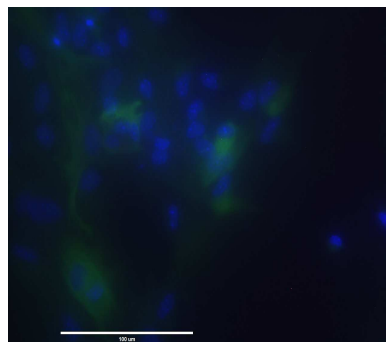


Figure 9: Nestin immunostaining showing NSCs in co-cultures in hypoxic conditions. DAPI (blue) staining shows nuclei.

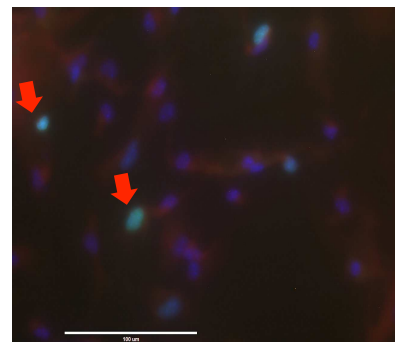
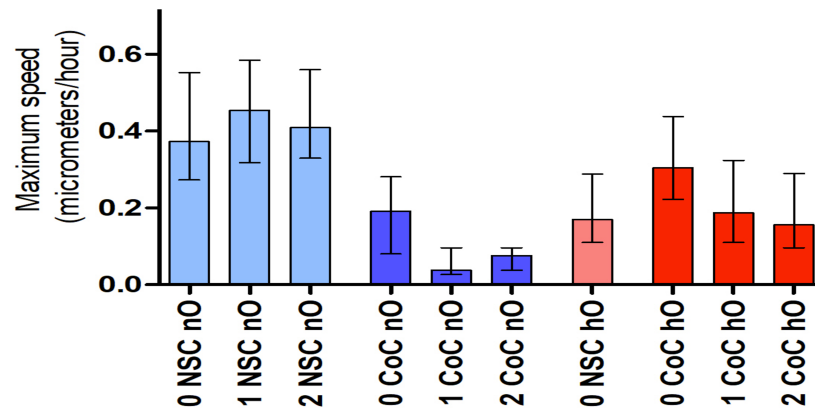


Figure 10: Nestin immunostaining showing NSCs and presence of Ki67 positive cells (red arrow) in co-cultures in hypoxic conditions.

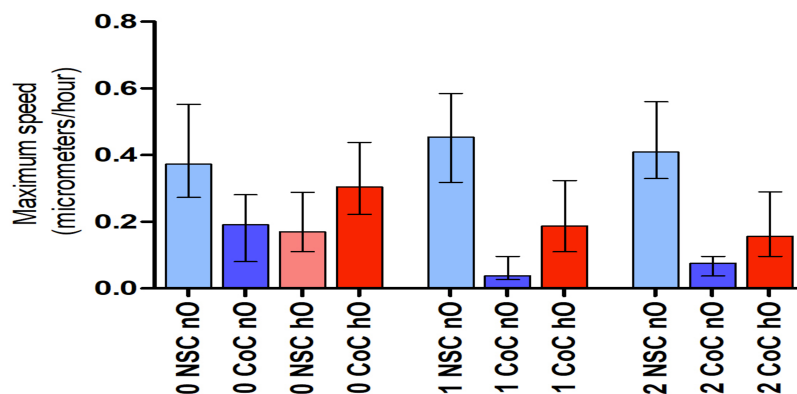
8.4. Quantification of cellular motility in normoxia and hypoxia

NSCs were tracked until their differentiation into neurons and afterwards neurons (NSCs-neurons) were tracked in single cultures and co-cultures. Astrocytes were not traced because there was no appreciable movement due to their attachment to the surface.

Maximum speed: Maximum speed (graph 1) of migration was compared between NSCs-neurons (control) and NSCs-neurons in astroglial-neuronal co-cultures in normoxia and hypoxia. The maximum speed was highest in NSCs-neurons alone in normoxia while lowest speed was observed in hypoxia. Surprisingly, there was significant decline in maximum speed of NSCs-neurons in astroglial-neuronal co-cultures as compared to NSCs-neurons alone in normoxic conditions, and as compared to NSCs-neurons in co-cultures in hypoxia. Day to day comparison (graph 2) demonstrated that the maximum speed was highest on day of seeding in almost all groups and decreased in following days. There was no significant difference in maximum speed of NSC-neurons alone for three days while it decreased from day 0 to onwards in rest of the groups. The results of statistical analysis of maximum speed comparison are given in Table 1.

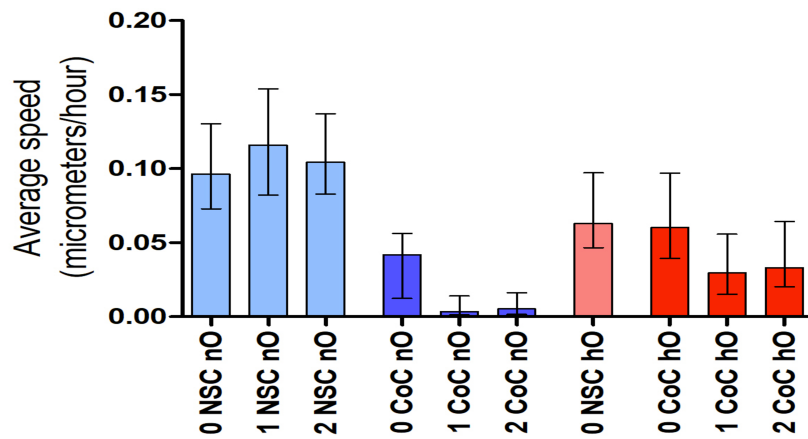


Graph 1: Comparison of maximum speed of NSCs-neurons in different groups. NSC (neuronal stem cells) CoC (astroglial-neuronal co-cultures), 0,1,2 (Days), nO (normoxia), hO (hypoxia)

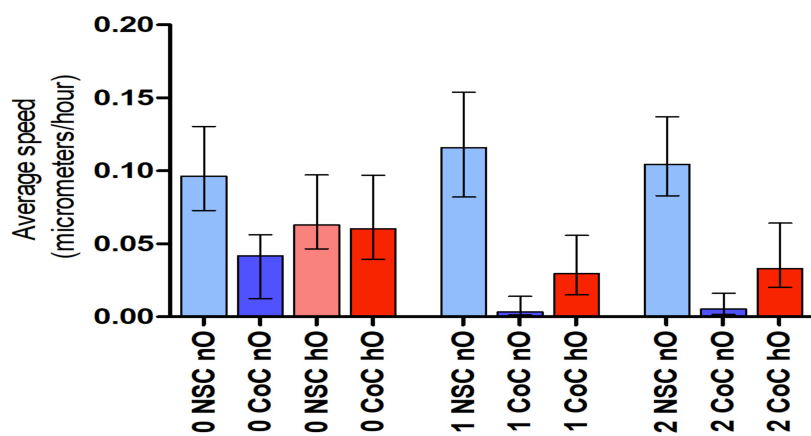


Graph 2: Comparison of maximum speed of NSCs-neurons by days in groups. NSC (neuronal stem cells) CoC (astroglial-neuronal co-cultures), 0,1,2 (Days), nO (normoxia), hO (hypoxia)

Average speed: Comparison of average speed of NSCs-neurons (control) and NSCs-neurons in astroglial-neuronal co-cultures in normoxic and hypoxic conditions is presented in graph 3. The average speed almost followed the same trend as maximum speed except of NSCs-neurons alone in hypoxic conditions. The average speed of NSCs-neurons alone in hypoxic conditions was higher than in astroglial-neuronal co-cultures in both normoxic and hypoxic conditions; however, it was not significant (Table 1). The highest average speed was of NSCs-neurons alone in normoxic condition while lowest was in astroglial-neuronal co-cultures in normoxic conditions. Day to day comparison (graph 2) showed same pattern as the maximum speed, which was highest on the day of seeding in almost all groups and it decreased in following days. Once again there was no significant difference in average speed of NSC-neurons alone for three days while it decreased from day 0 to onwards for rest of the groups. The results of statistical analysis of average speed comparison are given in Table 1.

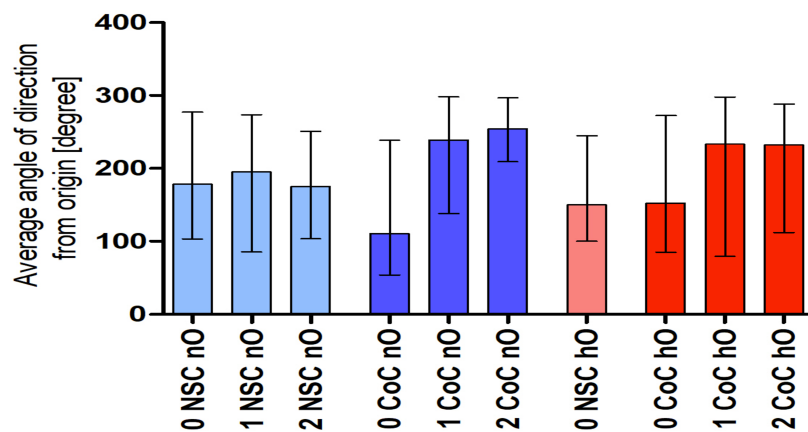


Graph 3: Comparison of average speed of NSCs-neurons in different groups. NSC (neuronal stem cells) CoC (astroglial-neuronal co-cultures), 0,1,2 (Days), nO (normoxia), hO (hypoxia)

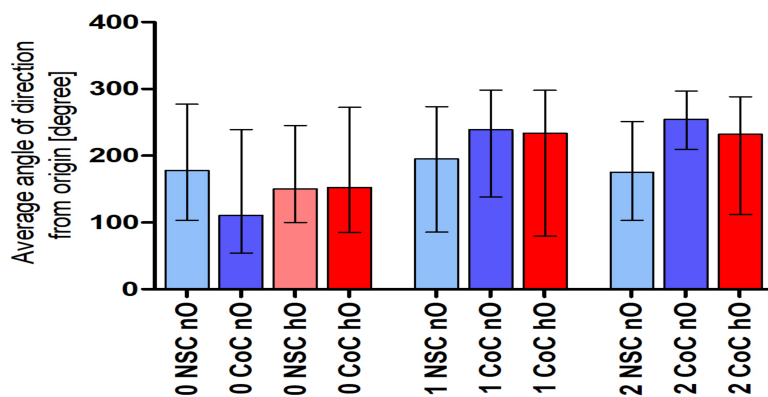


Graph 4: Comparison of average speed of NSCs-neurons by days in different groups. NSC (neuronal stem cells) CoC (astroglial-neuronal co-cultures), 0,1,2 (Days), nO (normoxia), hO (hypoxia)

Average angle of direction from origin: Graphs 5 shows comparison of average angle of direction from origin of NSCs-neurons alone (control) and of NSCs-neurons in astroglial-neuronal co-cultures. There was higher average angle of direction from origin in co-cultures as compared to single cultures. There was no significance difference among different groups in both normoxic and hypoxic conditions. Day to day comparison (graph 6) of average angle of direction from origin indicated a different trend than maximum speed and average speed. There was increase in average angle of direction from origin from day 0 to day 3 in all groups; however, it was not statistically significant. The only statistically significant difference was in day 2 between NSCs-neurons alone and NSCs-neurons of astroglial-neuronal co-cultures in normoxic conditions. There was also no significantly difference in average angle of direction from origin in each group for different days, except of difference between day 0 and day1, 2 of astroglial-neuronal co-cultures in normoxic conditions (Table 1). The results of statistical analysis of this comparison are presented in Table 1.



Graph 5: Comparison of average angle of direction from origin of NSCs-neurons in different groups. NSC (neuronal stem cells) CoC (astroglial-neuronal co-cultures), 0,1,2 (Days), nO (normoxia), hO (hypoxia)



Graph 6: Comparison of average angle of direction from origin of NSCs-neurons by days in different groups. NSC (neuronal stem cells) CoC (astroglial-neuronal co-cultures), 0,1,2 (Days), nO (normoxia), hO (hypoxia)

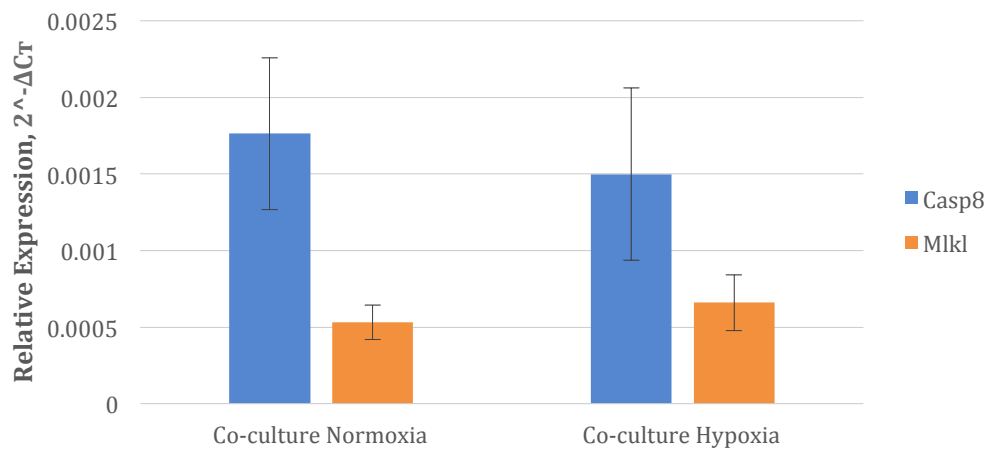
Statistical analysis of locomotion parameters: Nonparametric Kruskal-wallis and post-hoc Dunn's test for multiple comparisons were performed for maximum speed, average speed and average angle of direction from origin. For all the tests, $p < 0.05$ was considered significant.

Comparison between different conditions	Maximum speed Significant? $p < 0.05$	Average speed Significant? $p < 0.05$	Average angle of direction from origin Significant? $p < 0.05$
NSCs normoxia day 0 vs. NSCs hypoxia day 0	+	+	-
NSCs normoxia day 0 vs. Co-cultures normoxia day 0	+	+	-
NSCs normoxia day 0 vs. Co-cultures hypoxia day 0	-	+	-
NSCs normoxia day 1 vs. Co-cultures normoxia day 1	+	+	-
NSCs normoxia day 1 vs. Co-cultures hypoxia day 1	+	+	-
NSCs normoxia day 2 vs. Co-cultures normoxia day 2	+	+	+
NSCs normoxia day 2 vs. Co-cultures hypoxia day 2	+	+	-
Co-cultures normoxia day 0 vs. NSCs hypoxia day 0	-	+	-
Co-cultures normoxia day 0 vs. Co-cultures hypoxia day 0	+	+	-
Co-cultures normoxia day 1 vs. Co-cultures hypoxia day 1	+	+	-
Co-cultures normoxia day 2 vs. Co-cultures hypoxia day 2	+	+	-
Co-cultures hypoxia day 0 vs. NSCs hypoxia day 0	+	-	-
Comparison within each condition			
NSCs normoxia day 0 vs. NSCs normoxia day 1	-	-	-
NSCs normoxia day 0 vs. NSCs normoxia day 2	-	-	-
NSCs normoxia day 1 vs. NSCs normoxia day 2	-	-	-
Co-cultures normoxia day 0 vs. Co-cultures normoxia day 1	+	+	+
Co-cultures normoxia day 0 vs. Co-cultures normoxia day 2	+	+	+
Co-cultures normoxia day 1 vs. Co-cultures normoxia day 2	-	-	-
Co-cultures hypoxia day 0 vs. Co-cultures hypoxia day 1	+	+	-
Co-cultures hypoxia day 0 vs. Co-cultures hypoxia day 2	+	+	-
Co-cultures hypoxia day 1 vs. Co-cultures hypoxia day 2	-	-	-

Table 1: Results of post-hoc Dunn's test for multiple comparisons. There was significant difference between maximum and average speed among different groups and within each group for different days as compared to average angle of direction from origin.

8.5. Relative expression of caspase 8 and MLKL in astroglial-neuronal co-cultures in normoxia and hypoxia

The relative expression of caspase 8 and MLKL in astroglial-neuronal co-cultures in both normoxic and hypoxic conditions is presented in graph 7. The results showed expression of both genes in co-cultures in both normoxic and hypoxic conditions. There was tendency of higher expression of caspase 8 in both conditions, and it was also inclined to express more in normoxic conditions as compared to hypoxic conditions. On the other hand, co-cultures in hypoxic conditions had slight predisposition to express more MLKL as compared to normoxic conditions.



Graph 7: Relative expression of caspase 8 and MLKL in astroglial-neuronal co-cultures in normoxic and hypoxic conditions.

9. Discussion

In the present study, a valuable culture method was provided to obtain astroglial-neuronal co-cultures from primary astrocytes and NSCs. It is critical to obtain pure primary astrocytes cultures with minimum contamination with other cells. The cortices of newborn pups have other cells such as microglia, oligodendrocytes and fibroblasts, which could grow in primary astrocytes cultures. This could prevent to have appropriate astroglial-neuronal co-cultures to study interaction of astrocytes and neurons. The method used in this study to isolate primary astrocytes has shown good results in previous studies to obtain pure astrocyte cultures with minimum cellular contamination (45). Astrocytes tend to attach to surface of flask and grow as monolayer, while the microglia grow freely on top of the astrocytes (43). Neurons die early due to lack of appropriate growth medium. Thus microglia, oligodendrocytes precursor cells (OPCs) and dead neurons in primary astrocytes culture were reduced with tapping the flasks and changing the culture medium after every three days. To further decrease cellular contamination in primary astrocytes culture, use of anti-mitotic compound called arabinose

cytosine (Ara-C) is reported to have good results (46). It reduces the rapidly dividing cells such as microglia and fibroblasts (47, 48). The astrocytes culture purity was confirmed with immunostaining GFAP for astrocytes. Non-GFAP positive cells can be quantified and contaminants can be estimated. This methodology does not identify presence of specific cells, but it is a faster and more economic method to determine the percentage of non-astrocytic cells in the culture. Alternatively, purity of astrocytic cultures can be confirmed with immunostaining selective markers for the most prominent cell contaminants. For instance, antibodies against ionized calcium binding adaptor molecule (Iba-1), olig2 and vimentin can be used to detect microglia, OPCs and fibroblasts respectively (45).

The neuronal differentiation of NSCs was well observed in both only NSCs cultures and in astroglial-neuronal co-cultures with neuronal differentiation medium. The presence of EGF and FGF-2 are important to keep pluripotency of NSCs; thus, neuronal differentiation was seen after removal of these growth factors from full NSCs culture medium (49). Neurons with unipolar and bipolar morphology were present after 24 hours of seeding in both normoxic and hypoxic conditions. The neurons with this type of morphology are known to be sensory neurons.

Pyknosis, irreversible condensation of chromatin in the nucleus of a cell undergoing necrosis or apoptosis, was observed in NSC-neurons cultures in both normoxic and hypoxic conditions. It could be interesting to perform cell viability assay on NSCs cultures in both hypoxic and normoxic conditions to compare cell viability in these conditions. NSCs exist with in “physiological hypoxic” conditions at 1 to 5% O₂ in both embryonic and adult brains (50). Studies have shown that hypoxia promote the proliferation and differentiation of NSCs along with their survival in vitro and in vivo (50, 51). It is proposed that the mechanism of these responses might be primarily due to involvement of hypoxic inducible factor-1 (HIF-1) signaling pathway (50). HIF-1 when stabilized by hypoxic conditions, up regulates several genes to promote cell survival in low oxygen.

The astroglial-neuronal co-cultures in hypoxic conditions were assessed by immunocytochemistry. GFAP, nestin staining showed presence of astrocytes and NSCs respectively in co-cultures. Ki67 and nestin positive cells demonstrated presence of dividing NSCs. There was differentiation of NSCs to neurons; however, it was less robust than NSCs

single cultures. Studies have demonstrated that the molecules secreted from activated astrocytes increase proliferation and differentiation of NSCs (52). However, astrocytes in co-cultures were flat and epitheloid that resemble of immature astrocytes as compared to mature astrocytes that undergo hypertrophy and increased expression of GFAP in response to hypoxic condition (53). The presence of immature astrocytes in astroglial-neuronal co-cultures could be due to growth factors released by NSCs or there was differentiation of NSCs into immature astrocytes due to presence of fetal bovine serum in culture medium. The physical contact between astrocytes themselves and with neurons and NSCs was present. There was presence of syncytia between astrocytes. *In vivo* astrocytes form syncytia with other astrocytes and create highly intricate networks between several types of cells, including endothelial cells and neurons. This highly complex 3D network is not possible to mimic *in vitro* due to different morphology of astrocytes *in vitro* as compared to *in vivo* (54).

The quantification of locomotive parameters demonstrated superior cellular motility in astroglial-neuronal co-cultures in hypoxic conditions as compared to normoxic conditions in co-cultures and NSCs alone cultures. However, the highest cellular motility was of NSCs alone cultures in normoxic conditions. Cellular motility is dynamic process that is primarily driven by actin network beneath the cell membrane. The cellular motility observed in this study was of crawling type, which consisted of three components; protrusion of the leading edge, deadhesion of the cell body and cytoskeletal contraction to pull the cell forward (55). Cell motility is essential to variety of biological processes such as migration of the cells to the injury area. Studies have shown that in response to hypoxic-ischemic injury, NSCs migrates preferentially to the injury site and differentiate into neurons (56).

The better cellular motility in astroglial-neuronal co-cultures in hypoxic conditions as compared to in normoxic conditions could be due to changes in gene expression due to hypoxia. Hypoxia is shown to improve survival and growth of NSCs (51). Astrocytes also play an important role in guidance and support of neuronal migration during development and in response to injury (57). This was also observed in this study that there was tendency of higher average angle of direction from origin in astroglial-neuronal co-cultures as compared to single cultures. The higher average angle of direction from origin correlates with the movement towards a stimuli or chemoattractants. It is known that astrocytes release neurotrophic factors that act as chemoattractants for neuronal migration in response to injury

(57). The motility of NSCs is also important for transplantation therapy to repair damaged brain tissue. The transplanted NSCs preferentially migrate to the area of injury and differentiate into neurons (56). Thus, astroglial-neuronal co-cultures could provide a valuable tool to study the motility of NSCs and neurons as it incorporates affect of astrocytes, which is also present in vivo.

Necroptosis is a programmed form of necrotic cell death in caspase-independent fashion with leakage of cellular contents as compared to apoptosis, which is caspase-dependent, programmed cell death with no spilling of cellular contents. In necroptosis, the process of cell membrane permeabilization is tightly regulated that results in formation of necrosome via TNF α receptor signaling pathway. Necrosome then phosphorylates MLKL, which then insert into and permeabilize plasma membrane and organelles leading to leakage of cellular contents into the extracellular space (58). Necroptosis has been implicated in the pathology of ischemia-reperfusion injury in stroke and myocardial infarction (59).

The measurement of relative gene expression of apoptotic marker (caspase 8) and necroptosis marker (MLKL) revealed that process of apoptosis was higher than necroptosis in astroglial-neuronal co-cultures in normoxic and hypoxic conditions. There was tendency of low expression of caspase 8 in hypoxic conditions as compared to normoxic conditions. This could be due to protective affect of hypoxia on NSCs through HIFs). The slight higher inclination of necroptosis in hypoxic conditions as compared to normoxic conditions could be due to lack of energy in hypoxic conditions preferring less energy consuming process of necroptosis as compared to apoptosis. However, statistical analysis could not be performed on these differences in relative gene expression of caspase 8 and MLKL due to lack of NSCs and astrocytes in single cultures as biological controls.

Studies have shown substantial interplay between the apoptosis and necroptosis pathways. At multiple stages of their respective signaling cascades, the two pathways can regulate each other. Caspase 8 prevents the necroptosis by inhibiting the formation of necrosome, which is required to activate MLKL. Conversely, caspase 8 can be inactivated through anti-apoptotic protein CFLIP (60). Thus, there is reciprocal relationship between apoptosis and necroptosis. This reciprocal relationship was also observed in this study where relative gene expression of caspase 8 was higher than MLKL in both conditions.

10. Conclusion

Astrocytes have a substantial impact on the injury induced by an ischemic insult, thus suggesting that the crosstalk between glia and neurons is crucial to the neuronal protection in conditions of ischemia. This study helped to lay a foundation to develop an *in vitro* model of astroglial-neuronal co-cultures to study interaction of astrocytes and neurons in response to hypoxia. It is crucial to characterize the purity of these co-cultures, which is important to the correct interpretation of the results obtained. Quantifying cellular motility in cultures provided valuable information about the affect of hypoxic or normoxic conditions on NSCs, neurons and astrocytes, and also the affect of these cells on each other. The measurement of relative gene expression of caspase 8 and MLKL in astroglial-neuronal co-cultures provided valuable information about apoptosis and necroptosis in normoxic and hypoxic conditions. Thus, astroglial-neuronal co-cultures have the potential to obtain information about expression of genes involving astrocytes and neurons that play vital role in pathogenesis of hypoxic injury during ischemic stroke.

11. Acknowledgment

I would like to express my sincere gratitude to my mentor Prof. dr. sc. Dinko Mitrečić for giving me the opportunity to perform experimental work in his Laboratory for Stem Cells and for his continuous support of my thesis, for his patience, motivation, and immense knowledge. I would also like to thank Valentina Hribljan for her help in the laboratory work and Dunja Gorup for her guidance in statistical analysis of the results in this paper.

12. References

1. Feigin VL, Krishnamurthi RV, Parmar P, Norrving B, Mensah GA, Bennett DA, et al. Update on the global burden of ischemic and hemorrhagic stroke in 1990–2013: the GBD 2013 study. *Neuroepidemiology*. 2015;45(3):161-176. doi: 10.1159/000441085
2. Adams HP Jr, Bendixen BH, Kappelle LJ, Biller J, Love BB, Gordon DL, et al. Classification of subtype of acute ischemic stroke. Definitions for use in a multicenter clinical trial. TOAST. Trial of Org 10172 in Acute Stroke Treatment. *Stroke*. 1993;24(10):35-41.
3. Felberg RA, Burgin WS, Grotta JC. Neuroprotection and the ischemic cascade. *CNS Spectrums*. 2000;5:52-58.
4. Felberg, RA, Naidech, A. The five Ps of acute ischemic stroke treatment: parenchyma, pipes, perfusion, penumbra, and prevention of complications. *The Ochsner Journal*. 2003;1:5-11.
5. Wardlaw JM, Murray V, Berge E, del Zoppo GJ. Thrombolysis for acute ischaemic stroke. *Cochrane Database Systemic Review* 2014; 7: CD000213.
6. Whiteley WN, Emberson J, Lees KR, Blackwell L, Albers G, Bluhmki E, et al. Risk of intracerebral haemorrhage with alteplase after acute ischaemic stroke: a secondary analysis of an individual patient data meta-analysis. *Lancet Neurology* 2016;15:925-933.
7. Riedel CH, Zimmermann P, Jensen-Kondering U, Stingele R, Deuschl G, Jansen O. The importance of size: successful recanalization by intravenous thrombolysis in acute anterior stroke depends on thrombus length. *Stroke* 2011;42:1775-1777.
8. Boode B, Welzen V, Franke C, van Oostenbrugge R. Estimating the number of stroke patients eligible for thrombolytic treatment if delay could be avoided. *Cerebrovascular Diseases*. 2007;23(4):294-298. doi: 10.1159/000098330
9. Balami JS, Sutherland BA, Edmunds LD, Grunwald IQ, Neuhaus AA, Hadley G, et al. A systematic review and meta-analysis of randomized controlled trials of endovascular thrombectomy compared with best medical treatment for acute ischemic stroke. *International Journal of Stroke*. 2015;10:1168-1178.
10. Goyal, M, Yu, AYX, Menon, BK, Dippel, DWJ, Hacke, W et al. Endovascular therapy in acute ischemic stroke. *Stroke*. 2016;47:548-553.
11. Sutherland BA, Minnerup J, Balami JS, Arba F, Buchan AM, Kleinschnitz C. Neuroprotection for ischaemic stroke: translation from the bench to the bedside. *International Journal of Stroke* 2012;7:407-418.
12. Hoyte L, Barber PA, Buchan AM, Hill MD. The rise and fall of NMDA antagonists for ischemic stroke. *Current Molecular Medicine*. 2004;4(2):131-136.

13. Tu W, Xu X, Peng L, Zhong X, Zhang W, Soundarapandian MM, et al. DAPK1 interaction with NMDA receptor NR2B subunits mediates brain damage in stroke. *Cell*. 2010;140(2):222-234.
14. Pei L, Shang Y, Jin H, Wang S, Wei N, Yan H, et al. DAPK1-p53 interaction converges necrotic and apoptotic pathways of ischemic neuronal death. *Journal of Neuroscience*. 2014; 34(19):6546-6556.
15. Neuhaus AA, Couch Y, Hadley G, Buchan AM. Neuroprotection in stroke: the importance of collaboration and reproducibility. *Brain*. 2017;140(8):2079-2092. doi:10.1093/brain/awx126
16. Cook DJ, Teves L, Tymianski M. Treatment of stroke with a PSD-95 inhibitor in the gyrencephalic primate brain. *Nature*. 2012;483(7388):213-217. doi: 10.1038/nature10841
17. U.S. National Library of Medicine. Field Randomization of NA-1 Therapy in Early Responders (FRONTIER). [cited 2018 April 20]. Available from: <https://clinicaltrials.gov/ct2/show/NCT02315443>
18. Manzanero S, Santro T, Arumugam TV. Neuronal oxidative stress in acute ischemic stroke: sources and contribution to cell injury. *Neurochemistry International*. 2013;62(5):712-718.
19. Shuaib A, Lees KR, Lyden P, Grotta J, Davalos A, Davis SM, et al. NXY-059 for the treatment of acute ischemic stroke. *New England Journal of Medicine*. 2007;357:562-571.
20. Chamorro A, Amaro S, Castellanos M, Segura T, Arenillas J, Marti-Fabregas J, et al. Safety and efficacy of uric acid in patients with acute stroke (URICO-ICTUS): a randomised, double-blind phase 2b/3 trial. *Lancet Neurology*. 2014;13:453-460.
21. Feng S, Yang Q, Liu M, Li W, Yuan W, Zhang S, et al. Edaravone for acute ischaemic stroke. *Cochrane Database Systematic Review*. 2011;(12):CD007230. doi: 10.1002/14651858.CD007230.pub2.
22. Cramer SC, Chopp M, 2000. Recovery recapitulates ontogeny. *Trends in Neuroscience*. 2000;23:265-271.
23. Zhang ZG, Chopp M. Neurorestorative therapies for stroke: underlying mechanisms and translation to the clinic. *Lancet Neurology*. 2009;8:491-500.
24. Chopp M, Li Y, Zhang ZG. Mechanisms underlying improved recovery of neurological function after stroke in the rodent after treatment with neurorestorative cell-based therapies. *Stroke*. 2009;40(3):S143-145. doi: 10.1161/STROKEAHA.108.533141
25. Kalladka D, Sinden J, Pollock K, Haig C, McLean J, Smith W, et al. Human neural stem cells in patients with chronic ischaemic stroke (PISCES): a phase 1, first-in-man study. *Lancet*. 2016;388:787-96. doi: 10.1016/S0140-6736(16)30513-X

26. Cramer SC, Abila B, Scott NE, Simeoni M, Enney LA. Safety, pharmacokinetics, and pharmacodynamics of escalating repeat doses of GSK249320 in patients with stroke. *Stroke*. 2013;44(5):1337-1342. doi: 10.1161/STROKEAHA.111.674366.
27. Patel AR, Ritzel R, McCullough LD, Liu F. Microglia and ischemic stroke: a double edged sword. *International Journal of Physiology Pathophysiology Pharmacology*. 2013;5(2):73-90.
28. Biber K, Neumann H, Inoue K, Boddeke HW. Neuronal 'On' and 'Off' signals control microglia. *Trends in Neurosciences*. 2007;30(11):596-602.
29. David S. *Neuroinflammation: new insights into beneficial and detrimental functions*. John Wiley & Sons: Hoboken, New Jersey; 2015.
30. Stevens SL, Ciesielski TM, Marsh BJ, Yang T, Homen DS, Boule JL, et al. Toll-like receptor 9: a new target of ischemic preconditioning in the brain. *Journal of Cerebral Blood Flow Metabolism*. 2008;28(5):1040-1047. doi:10.1038/sj.jcbfm.9600606.
31. Hua F, Tang H, Wang J, Prunty MC, Hua X, Sayeed I, et al. TAK-242, an antagonist for Toll-like receptor 4, protects against acute cerebral ischemia/reperfusion injury in mice. *Journal of Cerebral Blood Flow Metabolism*. 2015;35(4):536-542. doi: 10.1038/jcbfm.2014.240.
32. Lampl Y, Boaz M, Gilad R, Lorberboym M, Dabby R, Rapoport A et al. Minocycline treatment in acute stroke: an open-label, evaluator-blinded study. *Neurology*. 2007;69:1404-1410.
33. Hayakawa K, Mishima K, Nozako M, Hazekawa M, Mishima S et al. Delayed treatment with minocycline ameliorates neurologic impairment through activated microglia expressing a high-mobility group box1-inhibiting mechanism. *Stroke*. 2008;39:951-958.
34. Lin JH, Weigel H, Cotrina ML, Liu S, Bueno E, Hansen AJ, et al. Gap-junction-mediated propagation and amplification of cell injury. *Nature Neurosciences*. 1998;6:494-500.
35. Stoll G, Jander S, Schroeter M. Inflammation and glial responses in ischemic brain lesions. *Progress in Neurobiology*. 1998;56(2):149-171.
36. Sliver J, Miller, JH. Regeneration beyond the glial scar. *Nature Reviews*. 2004;4:146-156.
37. Nedergaard M, Dirnagl U. Role of glial cells in cerebral ischemia. *Glia*. 2005;50:281-286.
38. Giffard RG, Swanson RA. Ischemia-induced programmed cell death in astrocytes. *Glia*. 2005;50(4):299-306.
39. Ouyang YB, Voloboueva LA, Xu LJ, Giffard RG. Selective dysfunction of hippocampal CA1 astrocytes contributes to delayed neuronal damage after transient forebrain ischemia. *Journal of Neuroscience*. 2007;27:4253-4260.

40. Xu L, Emery JF, Ouyang YB, Voloboueva LA, Giffard RG. Astrocyte targeted overexpression of Hsp72 or SOD2 reduces neuronal vulnerability to forebrain ischemia. *Glia*. 2010;58:1042-1049.
41. Roque C, Baltazar G. Impact of astrocytes on the injury induced by in vitro ischemia. *Cellular and Molecular Neurobiology*. 2017;37(8):1521-1528. doi: 10.1007/s10571-017-0483-3
42. Hao C, Richardson A, Fedoroff S. Macrophage-like cells originate from neuroepithelium in culture: characterization and properties of the macrophage-like cells. *International Journal of Developmental Neuroscience*. 1991;9(1):1-14.
43. Saura J. Microglial cells in astroglial cultures: a cautionary note. *Journal of Neuroinflammation*. 2007;4(26):1-11. doi:10.1186/1742-2094-4-26
44. Thermo Fisher Scientific. Gene expression analysis using real-time PCR. [cited on 2018 April 21]. Available from: <https://www.thermofisher.com/hr/en/home/life-science/pcr/real-time-pcr/real-time-pcr-applications/gene-expression-using-real-time-pcr.html>
45. Ferrer-Acosta, Y, Gonzalez-Vega MN, Rivera-Aponte DE, Martinez-Jimenez SM, Martins AH. Monitoring astrocytes reactivity and proliferation *in vitro* under ischemic-like conditions. *Journal of Visualized Experiments*. 2017;128: e55108.
46. Pont-Lezica L, Colasse S, Bessis A. Depletion of microglia from primary cellular cultures. *Methods in Molecular Biology*. 2013;1041:55-61.
47. Svensson M, Aldskogius H. Synaptic density of axotomized hypoglossal motor neurons following pharmacological blockade of the microglial cell proliferation. *Experimental Neurology*. 1993;120(1):123-131.
48. Wong VK, Shapourifar-Tehrani S, Kitada S, Choo PH, Lee DA. Inhibition of rabbit ocular fibroblast proliferation by 5-fluorouracil and cytosine arabinoside. *Journal of Ocular Pharmacology*. 1991;7(1):27-39.
49. Pollard SM, Conti L, Sun Yirui, Goffredo D, Smith A. Adherent neural stem (NS) cells from fetal and adult forebrain. *Cerebral Cortex*. 2006; 16(11):1377-1386.
50. Zhu LL, Wu LY, Yew DT, Fan M. Effects of hypoxia on the proliferation and differentiation of NSCs. 2005. *Molecular Neurobiology*. 2005;31:231-242.
51. Zhao T, Zhang CP, Zhu LL, Jin B, Huang X, Fan M. Hypoxia promotes the differentiation of neuronal stem cells into dopaminergic neurons. *Sheng Li Xue Bao*. 2007; 59(3):273-277.
52. Wang FW, Hao HB, Zhao SD, Zhang YM, Liu Q, Liu HJ et al. Roles of activated astrocytes in neural stem cells proliferation and differentiation. *Stem Cell Research*. 2011;17(1):41-53.
53. Rossi DJ, Brady JD, Mohr C. Astrocytes metabolism and signaling during brain ischemia. *Nature Neuroscience*. 2007;10(11):1377-1386.

54. Cornell-Bell AH, Finkbeiner SM, Cooper MS, Smith SJ. Glutamate induces calcium waves in cultured astrocytes: long-range glial signaling. *Science*. 1990; 247:470-473.
55. Ananthakrishnan R, Ehrlicher A. The forces behind cell movement. *International Journal of Biological Sciences*. 2007;3(5):303-317.
56. Park KL, Hack Ma, Ourednik J, Yandava B, Flax JD, Stiege PE et al. Acute injury directs the migration, proliferation of solid organ stem cells: evidence from the effect of hypoxia-ischemia in the CNS on clonal “reporter” neural stem cells. *Experimental Neurobiology*. 2006;199(1):156-178.
57. Kaneko N, Sawada M, Sawamoto K. Mechanisms of neuronal migration in the adult brain. *Journal of Neurochemistry*. 2017;141:835-847.
58. Wang H, Sun L, Su L, Rizo J, Liu L, Wang LF et al. Mixed lineage kinase domain-like protein MLKL causes necrotic membrane disruption upon phosphorylation by RIP3. *Molecular Cell*. 2014;54(1):133-146.
59. Zhou W, Yuan J. Necroptosis in health and diseases. *Seminars in Cell & Developmental Biology*. 2014;35:14-23.
60. Linkermann A, Green DR. Necroptosis. *The New England Journal of Medicine*. 2014;370(5):455-465.

13. Biography

Rana Tahir Rasool was born in Lahore, Pakistan. After finishing his high school in Pakistan, he went to Australia for higher education. He obtained his bachelor degree in Medical Sciences with major in Physiology and Neuroscience from Flinders University of South Australia. As part of graduate thesis for his bachelor degree, he performed experimental work to develop *in vitro* model to study interaction of astrocytes and microglia in response to focal cell death. He enrolled in Medicine Program at University of Zagreb, School of Medicine in 2012. In 2016, he was recipient of Amgen Scholars Research Program at University of Cambridge, U.K. During his scholarship at University of Cambridge, he worked on isolating neuronal stem cells of subependymal zone from cerebrospinal fluid. Currently, he is doing clinical elective in neurology and neurosurgery at National Hospital for Neurology and Neurosurgery, London. He has deep interest in research of neuronal repair after ischemic cell damage.